

Rubén Herrero-Illana, Miguel Ángel Pérez-Torres, Antxon Alberdi
Instituto de Astrofísica de Andalucía (IAA-CSIC)

A. Alonso-Herrero, L. Colina, A. Efstathiou, L. Hernández-García, D. Miralles-Caballero, P. Väisänen, C. Packham, V. Parjupaul, A. Zijlstra

The Luminous Infrared Galaxy NGC 1614 hosts a prominent circumnuclear ring of star formation. However, the nature of the dominant emitting mechanism in its central ~ 100 pc is still under debate. We present sub-arcsecond angular resolution radio, mid-infrared, Pa α , optical, and X-ray observations of NGC 1614, aimed at studying in detail both the circumnuclear ring and the nuclear region. We conclude that there is no need to invoke an AGN to explain the observed bolometric properties of the galaxy.

A multi-wavelength comparison

Our main aim is to shed light on the AGN/SB nature of the nuclear region of NGC1614. We discuss the striking morphological similarities between the radio and mid-IR images, which suggest a common origin for both emission mechanisms.

The most conspicuous feature is the prominent mid-IR emission of the nucleus, N, which contrasts with its rather faint emission at radio wavelengths (see Fig. 1). The regions to the northwest of the ring, A and B, show a mid-IR/radio ratio below the average of the whole ring (R), while regions C and D show the opposite behavior.

The nuclear region, N, shows a non-thermal spectral index of $\alpha \sim -1.80$. Such a steep spectral index seems to be at odds with an AGN origin for the radio emission of region N, but can be reconciled with the scenario of a compact starburst. The radio spectral index is the average value over region N, of ~ 90 pc in radius, so in principle we cannot rule out completely the existence of a hidden AGN inside that region, as found in other LIRGs, e.g., in Arp 299-A (Pérez-Torres et al. 2010). However, even if there is an AGN, its radio luminosity would not contribute more than $\sim 6\%$ and $\sim 7.6\%$ at 3.6 and 6.0 cm, respectively. Multi-wavelength diagnostic plots also locate NGC1614 in the starburst dominated region (Pérez-Olea & Colina 1996). Radio VLBI observations would provide the final diagnostic to completely exclude the presence of an AGN.

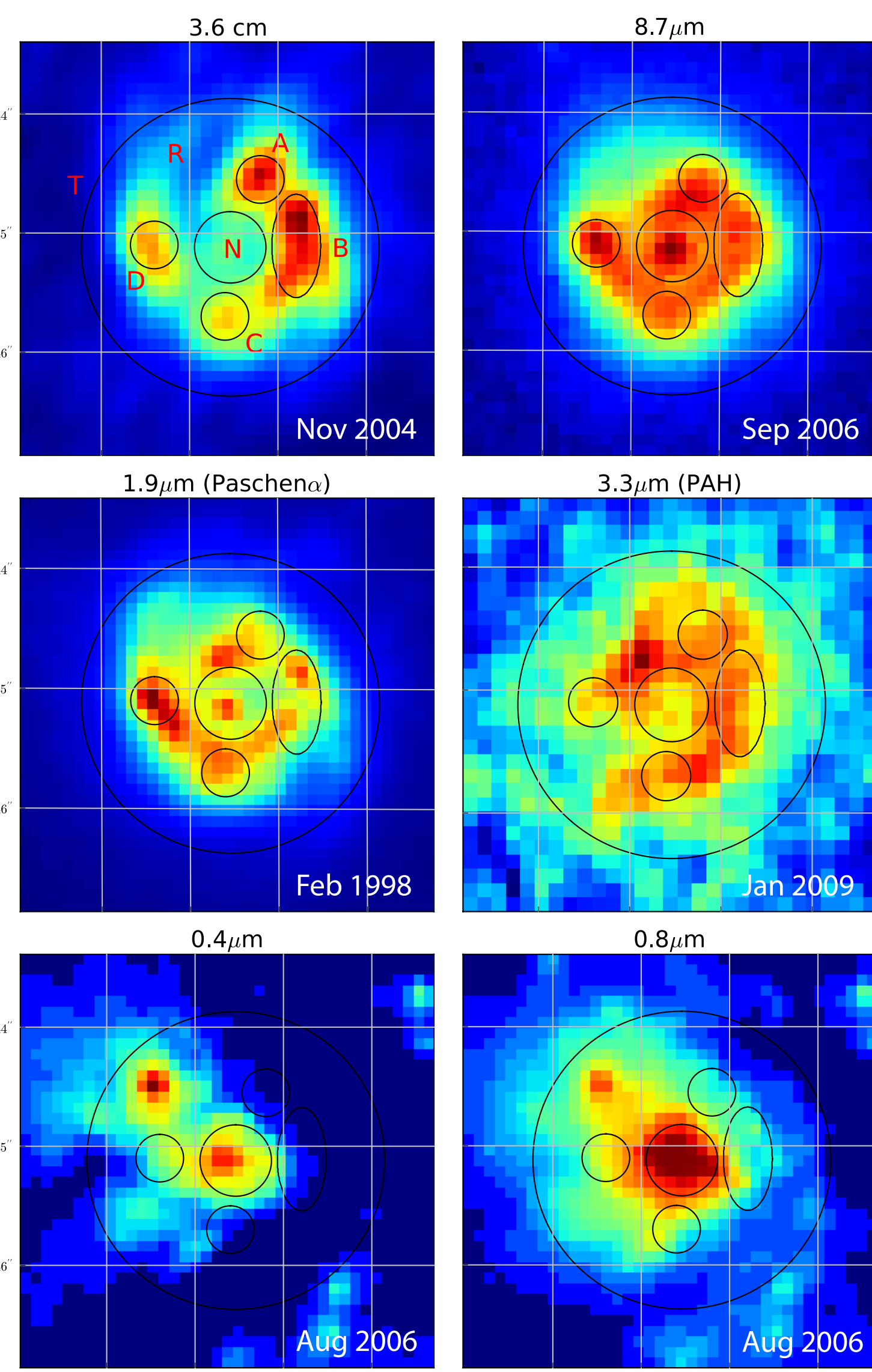


Fig. 1 - Multi-wavelength comparison of the nuclear region of NGC 1614. Based on the radio emission, we defined seven regions to compare the images, including the nuclear region (N), the whole ring (R), and the total area (T). Note the close similarity in the star formation ring and the contrast in the nuclear region between the radio and mid-IR wavelengths.

Radio thermal and non-thermal components

Massive stars and their associated HII regions are responsible for the thermal free-free radio emission, while SNe and SNRs account for the non-thermal synchrotron radio emission. Using extinction-corrected Pa α measurements, we inferred the amount of each type of radio emission. We found that:

$$S_{\text{thermal}} = 1.076 \times 10^{13} \times F(\text{Pa}\alpha) \nu^{-0.1}$$

The ratio of thermal free-free to synchrotron radio emission can be used as an indicator of the SB age of each region in the circumnuclear ring of NGC1614. The ratios of thermal to non-thermal radio emission (see Fig. 3) for regions A and B are about ~ 0.5 , while those of regions C and D of 1.1 and 1.2, respectively. The ratios above (and the free-free thermal continuum luminosities) can be well explained if the emission in regions C and D come from instantaneous bursts with ages < 5.5 Myr, where SNe have only recently started to explode. On the other hand, the emission from regions A and B would come from slightly older (~ 8 Myr) bursts. Since the thermal free-free emission is directly proportional to the Pa α flux, the decomposed images would indicate that the radio emission from the nuclear region is dominated by thermal free-free emission, which in turn suggests it is powered by a starburst, rather than an AGN.

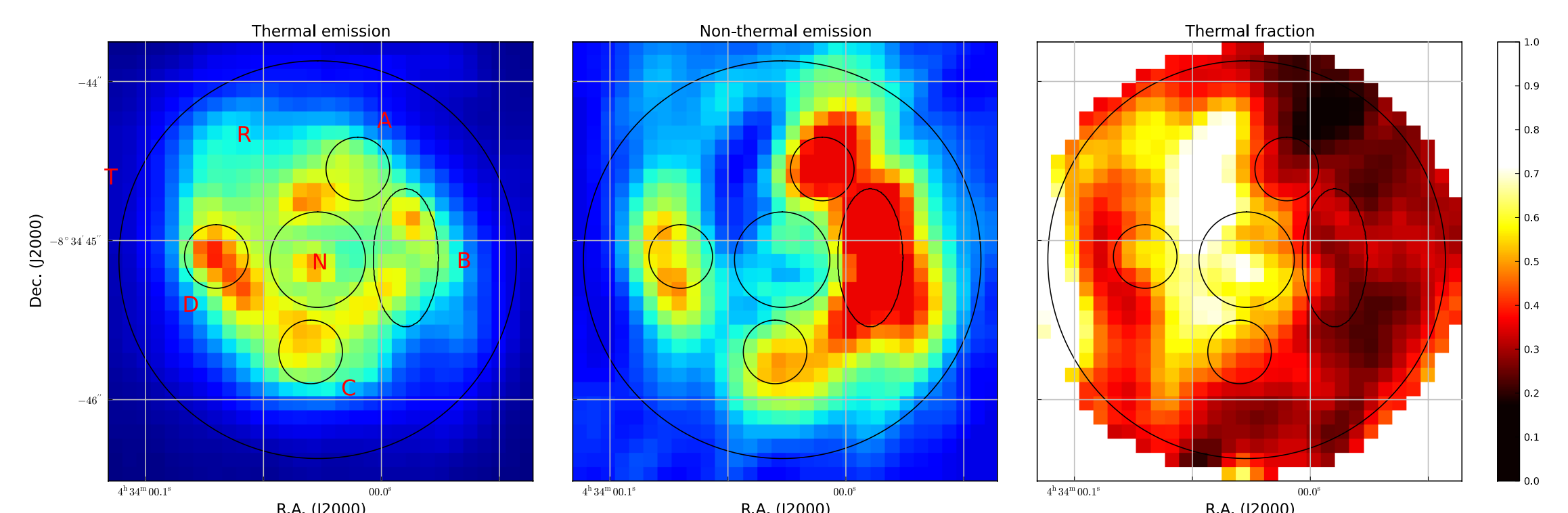


Fig. 3 - Decomposition of the 3.6 cm flux of the central region of NGC1614 into radio thermal (left) and non-thermal (middle) components. The right panel shows the relative contribution of the thermal emission.

Spatially Resolved X-ray Emission

We fitted the *Chandra* spectrum using four different models: (1) a pure thermal model (MEKAL), where the thermal emission is responsible for the bulk of the X-ray energy distribution; (2) an absorbed PL model, which corresponds to a non-thermal source representing an AGN; (3) a composite of a thermal plus an absorbed PL model (MEPL); and (4) a thermal model with tuned individual abundances (VMEKAL), which models the metal abundance pattern of type II SNe. Our best fit turned out to be the VMEKAL, giving support to the idea of a pure starburst model. This model finds abundances for Mg XI (1.36 keV), Si XIII (1.85 keV), and S XV (2.4 keV). The corresponding luminosity in the soft band for this model is $\log L(0.5-2 \text{ keV}) = 40.78 \text{ erg s}^{-1}$.

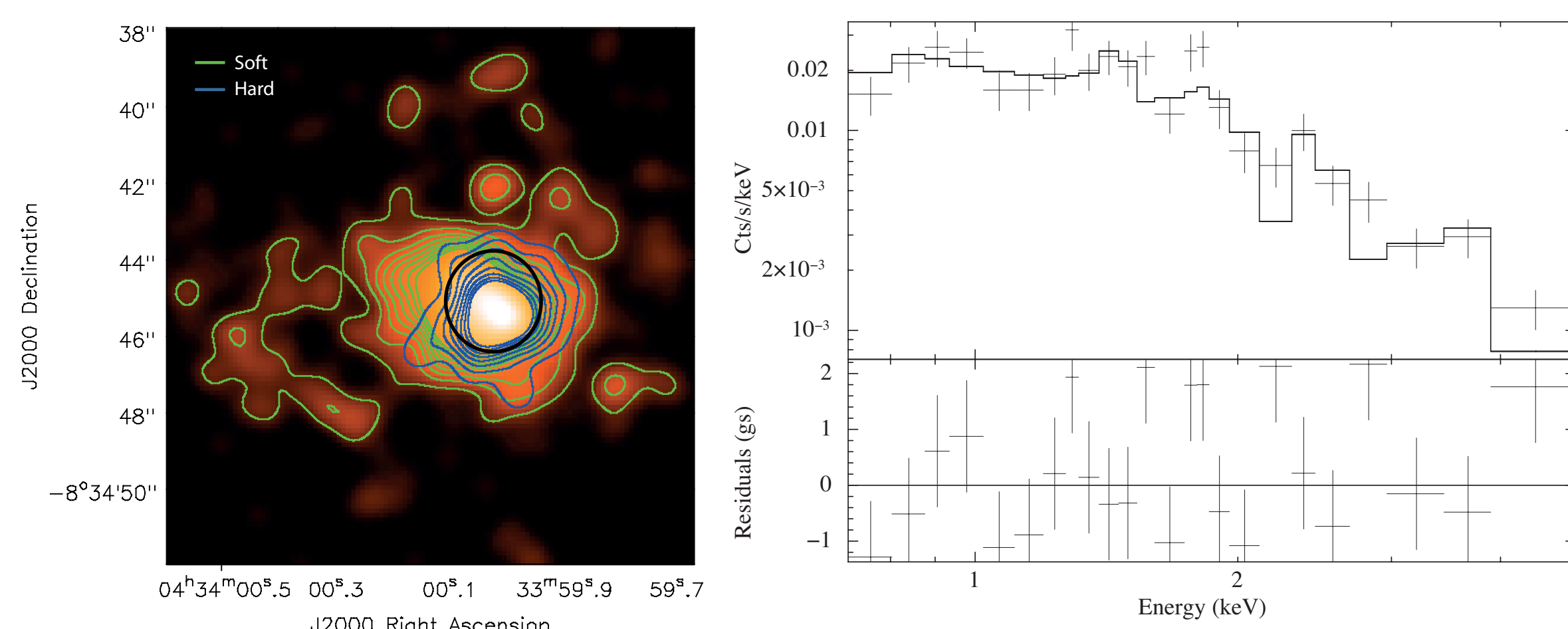


Fig. 2 - Chandra map and spectrum fit

SED model fit

We modeled NGC1614 SED using an exponentially decaying starburst model, by combining pure SB models from Efstathiou et al. (2009) and models from the host galaxies (Bruzual & Charlot, 2003). The model yields a bolometric luminosity of $10^{11.39} L_{\odot}$, an initial SFR of $85.1 M_{\odot} \text{ yr}^{-1}$, a core collapse supernova rate of 0.43 SN yr^{-1} , and an ionizing photon flux of $3.47 \times 10^{54} \text{ s}^{-1}$. The contribution of the AGN to the total bolometric luminosity, if any, would be in any case $< 10\%$.

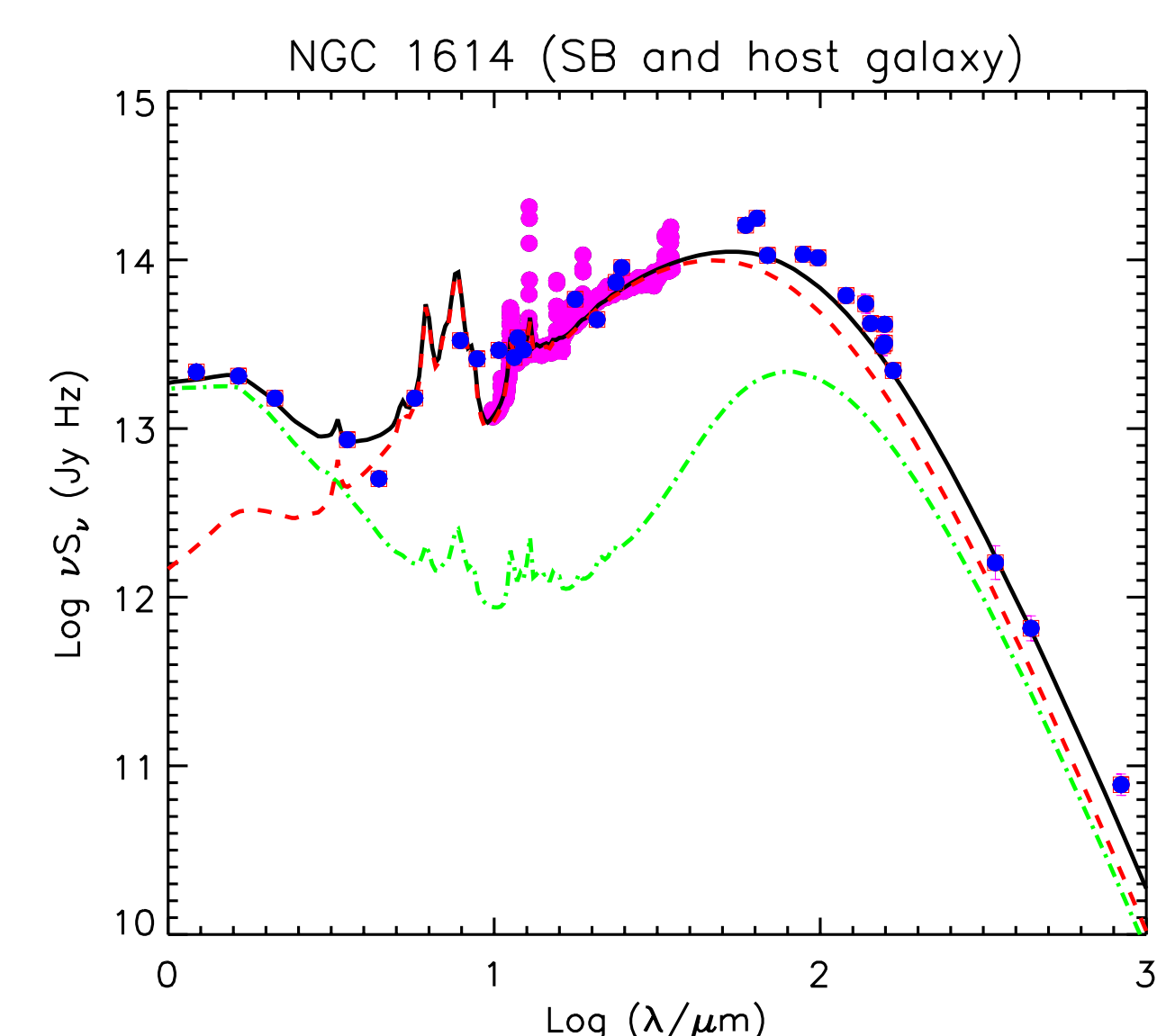


Fig. 4 - NGC1614 SED fitting. Photometric points are plotted in blue and pink. Lines show the overall fit (solid black), the starburst contribution (dashed red), and the host galaxy contribution (dot-dashed green). There is no need to include an AGN component

